

Extension of the Bonn meson exchange NN potential above pion production threshold: Nucleon renormalization and unitarity

Ch. Elster, W. Ferchländer, K. Holinde,* and D. Schütte

Institut für Theoretische Kernphysik, Universität Bonn, D-5300 Bonn, Federal Republic of Germany

R. Machleidt

Los Alamos National Laboratory, Los Alamos, New Mexico 87545

(Received 22 October 1986)

Nucleon self-energy diagrams, which are necessary to satisfy unitarity in NN scattering above pion production threshold, are studied for a realistic one-boson-exchange model. It is demonstrated that, in the framework of noncovariant perturbation theory, the independent iteration of (lowest order) bubble diagrams at both nucleon lines leads to dressing factors which provide well-defined off-shell corrections to the meson exchange contributions. It turns out that nucleon dressing yields additional attraction in lower partial waves. A slight readjustment of meson parameters (especially a reduction of the cutoff mass in the πNN vertex) leads to a reproduction of the empirical NN data below pion threshold which is of the same quality as before. The resulting inelasticities are, however, much too small, which clearly establishes the need for using a NN potential model containing the Δ isobar explicitly.

I. INTRODUCTION

It is generally accepted that quantum chromodynamics (QCD) is the fundamental theory of strong interactions. Therefore, the nucleon-nucleon (NN) interaction is completely determined by the underlying dynamics of the basic constituents, i.e., quarks and gluons. However, due to the nonperturbative character of QCD in the low-energy regime relevant for nuclear physics, we are far away from a quantitative understanding of the nuclear force in this way. Moreover, there is a good chance that conventional hadrons like nucleons, Δ isobars, and mesons, while being manifestations of the quark structure of matter, remain the relevant degrees of freedom for a wide range of nuclear physics phenomena. In that case, the overwhelming part of the force can be constructed in terms of meson-baryon vertices, which represent a natural and effective description of a complicated multi-quark reaction.

Recently, the Bonn group has presented a meson-exchange model of the NN interaction¹ for application below the pion production threshold, which is solely based on suitable meson-nucleon-nucleon and meson-nucleon- Δ isobar vertices W_α . The Hamiltonian $H = H_0 + W$ is treated in time-ordered perturbation theory. The resulting (energy-dependent) quasipotential V contains, in addition to single-meson exchange, explicit 2π -exchange contributions consistent with results obtained from dispersion theory (Paris potential²). Furthermore, it was essential to include corresponding $\pi\rho$ -exchange diagrams in order to obtain a quantitative fit to the NN data. In fact, these contributions ($2\pi + \pi\rho$) replace to a large extent the fictitious σ exchange used in former one-boson-exchange (OBE) models.

The extremely good reproduction of the empirical NN data with this model proves the usefulness of the meson

exchange picture as an effective description of the low-energy NN interaction. In order to further check its validity the same vertices should now be used consistently in the description of other hadronic processes (e.g., those involving strange particles, i.e., $KN, \Lambda N$) and in the evaluation of three-body forces and meson-exchange currents. Furthermore, the vertex parameters (coupling constants, cutoff masses), which have been fixed by adjusting them to the two-body data, can be checked against information from quark-gluon models. Finally, it is essential to extend the model of Ref. 1 above the pion production threshold. This, however, cannot be done in a straightforward way since the energy dependence of the (time-ordered) meson propagators leads to direct meson production. (Note that the use of static propagators does not include this possibility.) In order to still guarantee unitarity, nucleon (and Δ -isobar) self-energy diagrams (which, so far, have only roughly been taken into account by using empirical masses, see Ref. 1) must now be included explicitly for the following reason:³ In the three-particle (NN π) sector, unitarity of the S matrix implies for the scattering amplitude T :

$$i(T_{22} - T_{22}^\dagger) = T_{22} T_{22}^\dagger + T_{23} T_{23}^\dagger. \quad (1.1)$$

Here T_{22} is the elastic (NN), T_{23} is the π -production amplitude, and T_{23}^\dagger is the π -absorption amplitude. It is important to realize that self-energy diagrams involving π exchange are built up by $T_{23} T_{23}^\dagger$ and thus contribute, via Eq. (1.1), to $\text{Im} T_{22}$.

The total cross section is obtained from $\text{Im} T_{22}$, the elastic cross section from $|T_{22}|^2$. Since $T_{23} T_{23}^\dagger$ is positive definite, Eq. (1.1) implies the (weaker) unitarity bound

$$\sigma_{\text{total}} > \sigma_{\text{elastic}} \quad (1.2)$$

in the inelastic region.

In this paper, we want to study self-energy effects arising from the dressing of the nucleon. This step is relatively simple since it can be treated on the OBE level. Nevertheless, it has sufficient structure in order to get insight into the characteristic features and problems encountered in renormalization.

The basic concepts of our renormalization procedure are introduced in Sec. II. Some details concerning our numerical approach will be given in Sec. III. The results will be presented and discussed in Sec. IV. Especially, the following questions will be addressed.

- (i) Does the inclusion of explicit nucleon renormalization in the OBE picture still allow for a good reproduction of the empirical data below pion threshold?
- (ii) What is the effect of nucleon renormalization on the data above pion threshold, especially on the inelasticities?

II. NUCLEON RENORMALIZATION WITHIN AN OBE MODEL

In a one boson exchange model, we start from a Hamiltonian

$$\begin{aligned} H &= H_0^0 + W, \\ H_0^0 &= \sum_{\alpha} E_{\alpha}^0 a_{\alpha}^{\dagger} a_{\alpha} + \sum_n \omega_n b_n^{\dagger} b_n, \\ W &= \sum_{\alpha'an} W_{\alpha'an}^0 a_{\alpha}^{\dagger} a_{\alpha} b_n + \text{H.c.} \end{aligned} \quad (2.1)$$

a_{α}^{\dagger} and b_n^{\dagger} represent the creation operators for nucleons and bosons, respectively. $W_{\alpha'an}^0$ describe the nucleon-nucleon-meson vertices with unrenormalized coupling constants and form factors, whose presence is dictated by the extended hadron structure. Antinucleons are left out, for good reasons. Both chiral invariance and quark model arguments⁴ require that the $\text{NN}\bar{\text{N}}$ vertex is considerably suppressed compared to the NN vertex. Thus, there is only nucleon renormalization in the model; E_{α}^0 stands for the energy of the bare nucleon.

A perturbation expansion of the Hamiltonian (2.1) gives, apart from conventional meson exchange processes, self-energy contributions to the nucleon propagator up to infinite order in the coupling constant; some lower order diagrams of this expansion are shown in Fig. 1. Since we want to restrict ourselves to quasipotential contributions of one-boson-exchange type, which are of second order in the coupling constant and contain only three-particle (nucleon-nucleon-boson) cuts, it would be

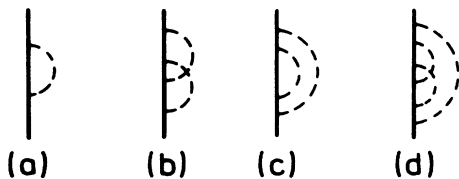


FIG. 1. Nucleon self-energy corrections of various orders in the coupling constant.

inconsistent to consider higher order contributions to the nucleon self-energy [Figs. 1(b)–(d)] explicitly. Therefore, we include in our model only iterated one-loop corrections to the nucleon propagator [Fig. 1(a)]. (In fact, higher order diagrams are to some extent taken into account by using the physical, renormalized mass for the intermediate nucleon state.) In addition, since the threshold for production of mesons other than the pion is quite high, we will consider only one-loop diagrams involving the pion.

Renormalization involving one-loop corrections only is exactly solvable in the framework of the Lee model and has been studied extensively.^{5–8} We want, at this point, only give those results, which are relevant for our model. Taking into account the self-energy diagram of Fig. 1(a) leads to the physical, renormalized nucleon energy E_{α} given by

$$E_{\alpha} = E_{\alpha}^0 + h_{\alpha}(E_{\alpha}), \quad (2.2)$$

where the mass operator is given by

$$h_{\alpha}(E_{\alpha}) = \sum_{\beta n} \frac{|W_{\alpha\beta n}^0|^2}{E_{\alpha} - E_{\beta} - \omega_n}. \quad (2.3)$$

This allows one to write the Hamiltonian (2.1) in a more convenient way, namely that the free part contains physical, renormalized energies only

$$\begin{aligned} H &= H_0 + H_I, \\ H_I &= W - \delta E, \quad \delta E = \sum_{\alpha} h_{\alpha}(E_{\alpha}) a_{\alpha}^{\dagger} a_{\alpha}. \end{aligned} \quad (2.4)$$

The wave function of the dressed nucleon turns out to be

$$|\alpha\rangle^d = |\alpha\rangle + \sum_{\beta n} \frac{W_{\alpha\beta n}^{0*}}{E_{\alpha} - E_{\beta} - \omega_n} |\beta n\rangle. \quad (2.5)$$

($|\alpha\rangle = a_{\alpha}^{\dagger} |0\rangle$; $|\beta n\rangle = a_{\beta}^{\dagger} b_n^{\dagger} |0\rangle$, $|0\rangle$ being the vacuum state.) It is not normalized to 1 but

$${}^d\langle\alpha|\alpha\rangle^d = Z_{\alpha}^2(E_{\alpha}) = 1 + \sum_{\beta n} \frac{|W_{\alpha\beta n}^0|^2}{(E_{\alpha} - E_{\beta} - \omega_n)^2}. \quad (2.6)$$

Introducing renormalized matrix elements

$$W_{\alpha\beta n} = W_{\alpha\beta n}^0 / Z_{\alpha}(E_{\alpha}), \quad (2.7)$$

the wave function renormalization constant $Z_{\alpha}(E_{\alpha})$ reads

$$Z_{\alpha}^{-2}(E_{\alpha}) = 1 - \sum_{\beta n} \frac{|W_{\alpha\beta n}|^2}{(E_{\alpha} - E_{\beta} - \omega_n)^2}. \quad (2.8)$$

It should be noted that the matrix element $W_{\alpha\beta n}$ has to be chosen sufficiently small in order to ensure a positive norm of the free one-nucleon state $|\alpha\rangle^d$. This constraint imposes an upper limit on the $\text{NN}\pi$ form factor (see below). The correctly normalized wave function ψ_{α} of the one-nucleon state can then be written as

$$\psi_{\alpha} = Z_{\alpha}^{-1}(E_{\alpha}) |\alpha\rangle^d = [Z_{\alpha}^{-1}(E_{\alpha}) + \Omega_{\alpha}] |\alpha\rangle$$

with

$$(2.9)$$

$$\Omega_\alpha = \sum_{\beta n} \frac{W_{\alpha\beta n}^*}{E_\alpha - E_\beta - \omega_n} a_\beta^\dagger b_n^\dagger a_\alpha.$$

For solving the NN scattering problem we have to take into account that both nucleons have to be dressed simultaneously, which gives rise to three- and four-particle-cut contributions (Fig. 2). They can be formally handled in a Lee model framework, but require the introduction of an effective three-body potential for the four-particle-cut contributions.⁸ Alternatively, one could just suppress the dressing for one nucleon, as done by Kloet and Silbar.⁹ This asymmetric treatment, however, leads to problems with respect to the Pauli principle. Therefore, we will adopt the following procedure: We will keep the important symmetry between both nucleons by independently summing self-energy diagrams on both nucleon lines. On the other hand, we will neglect four-particle cut contributions to the dressing. (In fact, in a recent covariant study¹⁰ based on the Bethe-Salpeter equation, they have been shown to be quite small.)

Such a program can be achieved by starting with the following ansatz for the "free" two-nucleon channel state

$$|\alpha_1\alpha_2\rangle^d = (1 + \bar{\Omega}_{\alpha_1})(1 + \bar{\Omega}_{\alpha_2})|\alpha_1\alpha_2\rangle \quad (2.10)$$

($|\alpha_1\alpha_2\rangle \equiv a_{\alpha_1}^\dagger a_{\alpha_2}^\dagger |0\rangle$), where $\bar{\Omega}_{\alpha_1} \equiv Z_{\alpha_1}(E_{\alpha_1})\Omega_{\alpha_1}$ acts on nucleon 1 only and $\bar{\Omega}_{\alpha_2} \equiv Z_{\alpha_2}(E_{\alpha_2})\Omega_{\alpha_2}$ on nucleon 2, and $[\Omega_{\alpha_1}, \Omega_{\alpha_2}] = 0$ characterizing the independent summation of self-energy diagrams. The correctly normalized wave function can then be written as

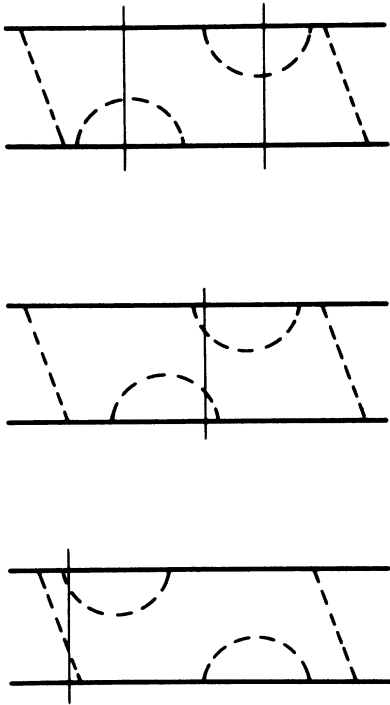


FIG. 2. Various contributions to three- and four-particle cuts in an NN iterative diagram containing nucleon self-energy contributions.

$$\psi_{12} = [Z_{\alpha_1}^{-1}(E_{\alpha_1}) + \Omega_{\alpha_1}][Z_{\alpha_2}^{-1}(E_{\alpha_2}) + \Omega_{\alpha_2}]|\alpha_1\alpha_2\rangle \quad (2.11)$$

which automatically ensures the correct normalization of the dressed one-nucleon state [see Eq. (2.9)].

The NN scattering states define a transition matrix

$$\langle \alpha'_1\alpha'_2 | T(E_{\alpha_1} + E_{\alpha_2} + i\epsilon) | \alpha_1\alpha_2 \rangle$$

which is the solution of a Lippmann-Schwinger-type equation

$$T(z) = V(z) + V(z) \frac{1}{z - h_0^{(N)}} T(z) \quad (2.12)$$

($h_0^{(N)}$ represents the free Hamiltonian with nucleons only). The quasipotential $V(z)$ is given by

$$\langle \alpha'_1\alpha'_2 | V(z) | \alpha_1\alpha_2 \rangle = R_{\alpha'_1\alpha'_2}(z) \bar{V}_{\alpha'_1\alpha'_2\alpha_1\alpha_2}(z) R_{\alpha_1\alpha_2}(z), \quad (2.13)$$

where \bar{V} denotes the usual meson-exchange potential [see, e.g., Ref. 1, Eqs. (B7)–(B10)]. This expression contains a two-particle dressing factor, symmetric in both nucleons,

$$R_{\alpha_1\alpha_2}^{-2}(z) = 1 - (z - E_{\alpha_1} - E_{\alpha_2})$$

$$\times \langle \alpha_1\alpha_2 | \Omega_{12}^\dagger \frac{1}{z - H_0} \Omega_{12} | \alpha_1\alpha_2 \rangle \quad (2.14)$$

($\Omega_{12} \equiv \Omega_{\alpha_1} + \Omega_{\alpha_2}$) which reduces to 1 at the on-shell point, as it should be. [In Ref. 8 it has been demonstrated that the independent summation of self-energy diagrams of the type of Fig. 1(a) leads to dressing factors as in Eq. (2.14). The only simplification adopted here is the neglect of four-particle contributions arising from the three-body interaction V_3 of Ref. 8.]

Furthermore, it should be emphasized that $V(z)$ contains renormalized quantities only. Therefore, it coincides at the pole of the NN T matrix with the standard boson exchange model.¹

The lowest-order diagrams contributing to $V(z)$ are shown in Fig. 3. Figures 3(a) and (b) represent the usual one-boson-exchange diagrams, Figs. 3(c)–(f) are the self-energy corrections due to the pion, which cancel on shell exactly.

Equation (2.14) can be evaluated as

$$R_{\alpha_1\alpha_2}^{-2}(z) = 1 - (z - E_{\alpha_1} - E_{\alpha_2}) \times [\Gamma_{\alpha_1}(z - E_{\alpha_2}) + \Gamma_{\alpha_2}(z - E_{\alpha_1})] \quad (2.15)$$

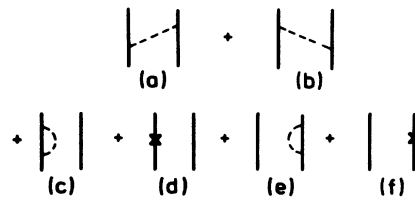


FIG. 3. Diagrams contributing to $V(z)$. The dashed line in (a) and (b) represents the exchange of all mesons, whereas in (c) and (d) the dashed line stands for the pion only.

with

$$\Gamma_{\alpha_i}(z - E_{\alpha_j}) = \sum_{\beta n} \frac{|W_{\alpha_i, \beta n}|^2}{(E_{\alpha_i} - E_{\beta} - \omega_n^\pi)^2 (z - E_{\alpha_j} - E_{\beta} - \omega_n^\pi)}. \quad (2.16)$$

Explicit formulas for the energy shift, the Z factor, and the dressing factor can be found in Appendix A.

$$T(q', q | 2E_q) = V(q', q | 2E_q) + \mathcal{P} \int_0^\infty \frac{dk k^2}{2E_q - 2E_k} V(q', k | 2E_q) T(k, q | 2E_q) - i \frac{\pi}{2} q E_q V(q', q | 2E_q) T(q, q | 2E_q). \quad (3.1)$$

The singularity for $k = q$ in the principal value integral is removed by subtracting the (zero-valued) integral

$$\mathcal{P} \int_0^\infty dk \frac{q^2 2E_q}{2(q^2 - k^2)} V(q', q | 2E_q) T(q, q | 2E_q). \quad (3.2)$$

The resulting integral equation with complex V and T is solved numerically as a coupled system for $\text{Re}T$ and $\text{Im}T$. The method proceeds analogously for angular-momentum coupled states.

The partial wave scattering amplitudes are related to the partial wave S matrix by

$$S_{L'L}^{JS}(E) = 1 + 2i T_{L'L}^{JS}(E). \quad (3.3)$$

$S_{L'L}^{JS}(E)$ can be parametrized as

$$S_{L'L}^{JS}(E) = \eta_{L'L}^{JS}(E) e^{2i\delta_{L'L}^{JS}(E)}, \quad (3.4)$$

where $\delta_{L'L}^{JS}(E)$ is the phase shift and $\eta_{L'L}^{JS}(E)$ the inelasticity parameter describing the absorption from the incident channel. Because of unitarity, $0 \leq \eta_{L'L}^{JS}(E) \leq 1$. In our actual calculations we mostly use the phase shift parametrization of Arndt and Roper.¹²

In purely elastic scattering the T -matrix equation has only one singularity, namely the pole of the two-nucleon propagator. Above pion production threshold, our (retarded) one-pion-exchange potential develops poles, which enter the scattering equation. Such poles are an expression of the fact that now real pions can be generated. However, they complicate things considerably and require an elaborate treatment, which is described in Appendix B.

IV. RESULTS AND DISCUSSION

Starting point of our calculations is a OBE model based on time-ordered perturbation theory. It is an updated version of Ref. 14; its meson parameters, given in Table I, have been fitted to the empirical data below pion production threshold. If this model is extended to the inelastic region the inelasticity parameter η , defined in Eq. (3.4) exceeds one in several low partial waves, indicating a violation of unitarity. This is illustrated in Fig. 4, for the 1S_0 and 3S_1 - 3D_1 partial waves in which the violation is largest. (A very similar result has been obtained by the authors of Ref. 10.) This unphysical feature is cured (up

III. T -MATRIX EQUATION AND PHASE SHIFTS

In order to obtain the helicity matrix elements of the NN transition amplitude, Eq. (2.12), we decompose it into partial wave amplitudes, for details see the review article of Erkelenz.¹¹ In contrast to Ref. 11, we do not introduce a K matrix since our potentials become complex above pion threshold. Thus, we now have for the uncoupled case the following T -matrix equation

to the second inelastic threshold) by including the lowest order (pion exchange) nucleon self-energy contributions of Figs. 3(c)–(f).

As mentioned already [see Eq. (2.8)] the inclusion of these self-energy corrections leads to a constraint for the pion form factor since the wave function renormalization factor must be positive. This condition implies an upper limit of Λ_π in the range of 1200 MeV if a monopole form factor at the vertex is used, see Table I. Of course, this number is due to our restriction to single-loop corrections; it should be expected to change when higher order terms like those in Figs. 1(b)–(d) were also included. For $\Lambda_\pi = 1200$ MeV we get $Z_q^{-2}(m) = 0.36$ (which means that the total nucleon wave function consists of 64% pion cloud) and a nucleon mass shift $Z_q^{-2}(m)h_q(m) = -817$ MeV.

Next we want to study the effect of nucleon dressing on the potential. Figure 5 shows the one-pion-exchange (OPE) potential $V^\pi(q', q | 2E_{q_0})$ in the 1S_0 state as a function of q for $q' = q_0 = 250$ MeV. Curve *a* is the original OPE potential calculated with the parameters of Table I. In a first step, we reduce the pion cutoff mass to $\Lambda_\pi = 1200$ MeV (curve *b*), which leads to a considerable suppression of the potential. Next, we include the dressing factor, Eqs. (2.15) and (2.16). On shell, i.e., for $q = q' = q_0$, the potential remains unchanged because $R_{q_0}^{-2}(2E_{q_0}) = 1$; for $q < q_0$ it is diminished, whereas for $q > q_0$ it is enhanced.

Since in the iteration of the OPE potential intermediate momenta q around 600 MeV play the dominant role, the

TABLE I. Meson parameters of the OBE model used in this paper. The number in parentheses denotes the tensor to vector ratio f_α/g_α . The form factor at the vertex is parametrized as $F_\alpha = \Lambda_\alpha^2 - m_\alpha^2 / \Lambda_\alpha^2 + \mathbf{k}^2$. Nucleon mass $m = 938.926$ MeV.

	$g_\alpha^2/4\pi$	m_α (MeV)	Λ_α (MeV)
π	14.4	138.03	1750
ρ	0.9 (6.1)	769	1500
ω	20	782.6	1500
σ	8.8819	550	2000
δ	1.0534	983	2000
η	5	548.8	1500

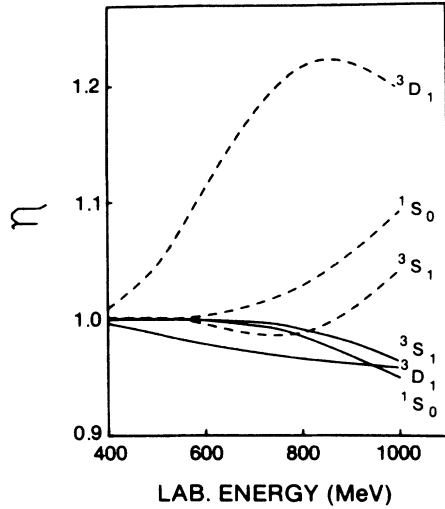


FIG. 4. Inelasticity parameter η in the inelastic region for various partial waves with (solid line) and without (dashed line) nucleon self-energy corrections.

dressing should enhance strongly higher iterations of the OPE potential. This is indeed the case, as shown in Fig. 6 for the second iteration. Obviously, the dressing enlarges it by about 30%. Furthermore, the reduced strength of the potential due to the smaller cutoff mass is nearly completely compensated by the nucleon dressing.

The influence of nucleon dressing on the total OBE potential is shown in Fig. 7. For small q the potential remains nearly unchanged whereas for large q the repulsion (mainly originating from ω exchange) is strongly enhanced.

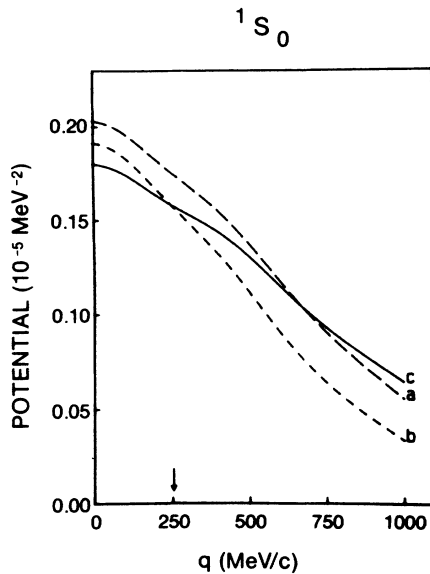


FIG. 5. One-pion-exchange potential $V^\pi(q', q | 2E_{q_0})$ in the 1S_0 state as a function of q for $q' = q_0 = 250$ MeV. Curve a is based on a cutoff mass $\Lambda_\pi = 1750$ MeV, whereas b is obtained with $\Lambda_\pi = 1200$ MeV. Curve c is the exchange potential (b) multiplied with the dressing factor $R_q^{-2}(z)$. The on-shell point is marked by an arrow. ($z = 2E_{q_0}$ is the starting energy.)

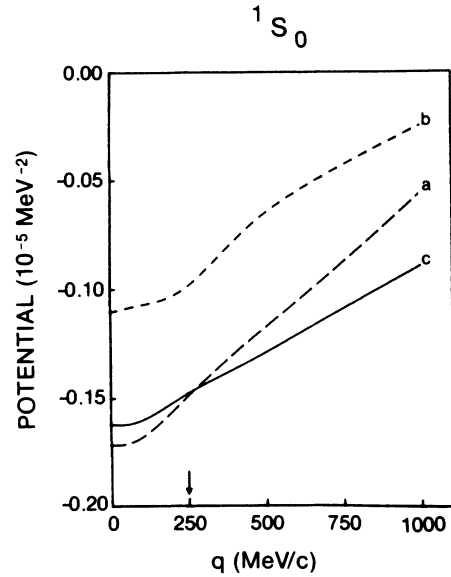


FIG. 6. Second iteration of the OPE potential $V^\pi(q', q | 2E_{q_0})$ in the 1S_0 state as function of q for $q' = q_0 = 250$ MeV. The notation is the same as in Fig. 5.

The effect of nucleon dressing on the NN partial wave phase shifts, obtained from a solution of the scattering equation (2.12), is shown in Fig. 8. Since it is an off-shell effect it is quite small in higher partial waves, e.g., 3G_4 . However, in lower partial waves, the nucleon dressing has a visible effect leading always to additional attraction, especially for higher energies. This is due to the fact that now the iterations of the potential become important, which are attractive and are increased by the dressing factor.

In the 3D_2 state, the effect of nucleon dressing is totally

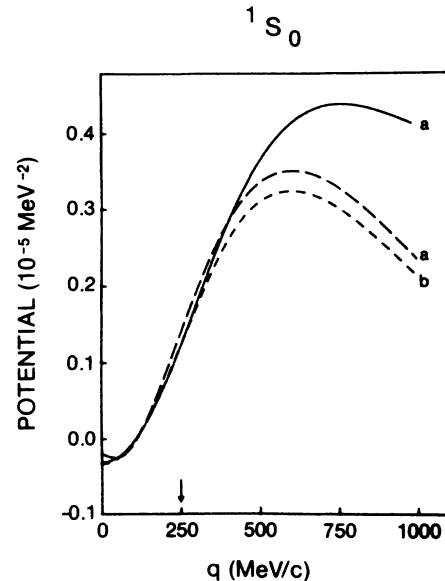


FIG. 7. One-boson-exchange potential $V^{OBE}(q', q | 2E_{q_0})$ in the 1S_0 state as function of q for $q' = q_0 = 250$ MeV. The notation is the same as in Fig. 5.

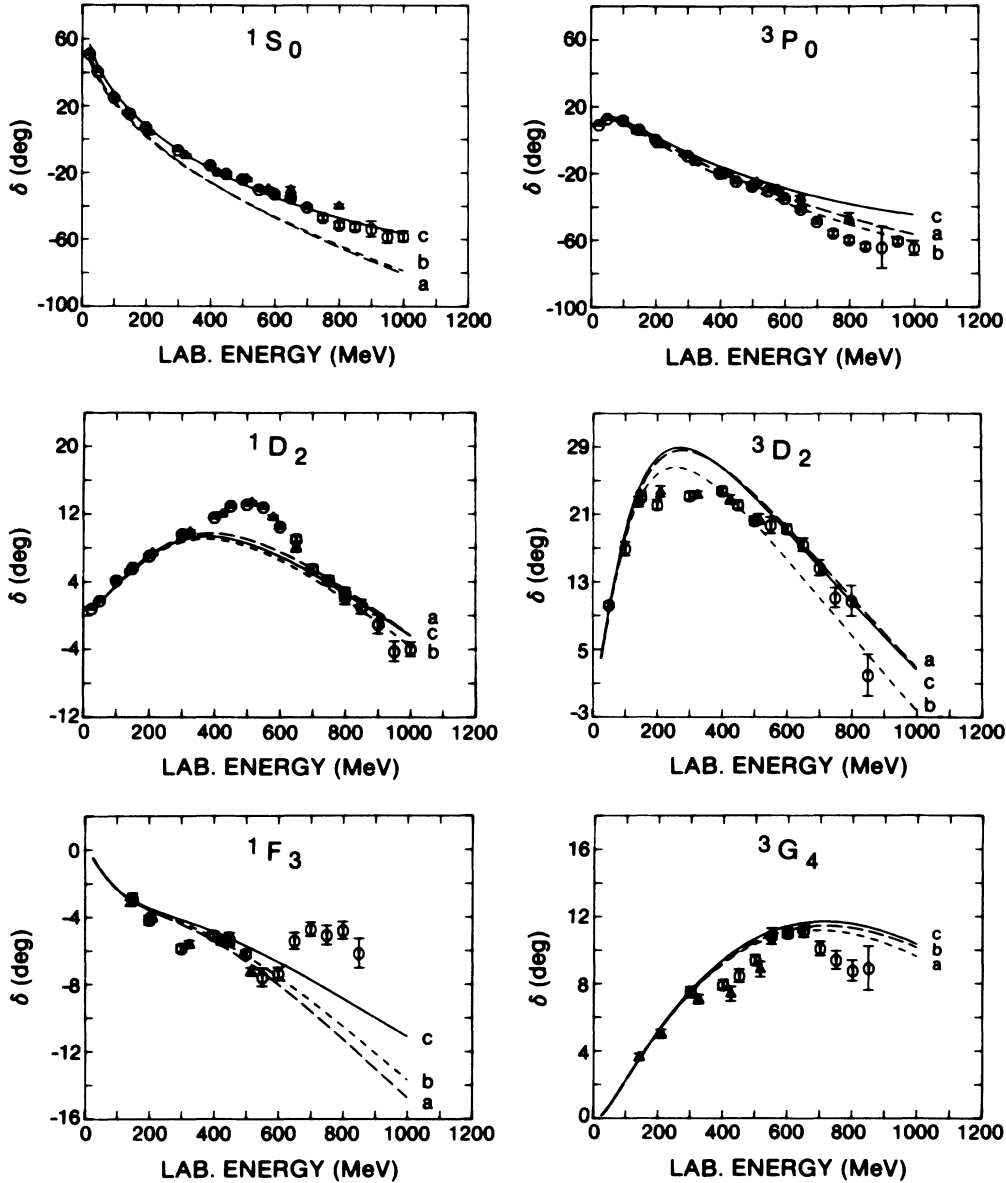


FIG. 8. NN phase shifts δ_{LSJ} (in degrees) as function of the nucleon lab energy derived from an OBE potential. The error bars are taken from Ref. 12 (open octagon) and Ref. 15 (open triangle). The notation is the same as in Fig. 5.

compensated by the use of a smaller Λ_π . On the other hand, due to the vanishing tensor force in the $1S_0$ state, the effect remains in that partial wave, leading to additional attraction necessary to describe the empirical data. The same effect has been found by Faassen.^{16,10}

The inelasticity parameters ρ_{LSJ} (defined in the Arndt-Roper convention) are shown in Fig. 9. In general, they are too small to fit the empirical data. This is to be expected because it is well known that pion production is mainly due to the decay of a Δ isobar (which is not contained in our OBE model). This is most clearly seen in the $1D_2$ state; also, the resonance structure of the corresponding real phase shift is missed completely. It remains however that, based on the present OBE model,

nucleon dressing is essential in order to have a unitary model above pion production threshold.

In order to show the combined effect of (a) nucleon dressing and (b) a lower value of Λ_π on the deuteron data we started from the OBE model including dressing [case (c)] and adjusted the meson parameters to fit the NN phase shifts as well as the deuteron binding energy quantitatively. It turns out that, compared to the original model which predicted a quadrupole moment $Q_D = 0.278$ fm² and a D -state probability $P_D = 4.19\%$, the quadrupole moment is now decreased by 0.007 fm², mainly due to the smaller pion cutoff mass. On the other hand, P_D is increased by about 0.1%, showing that the effect of nucleon dressing dominates at shorter ranges.

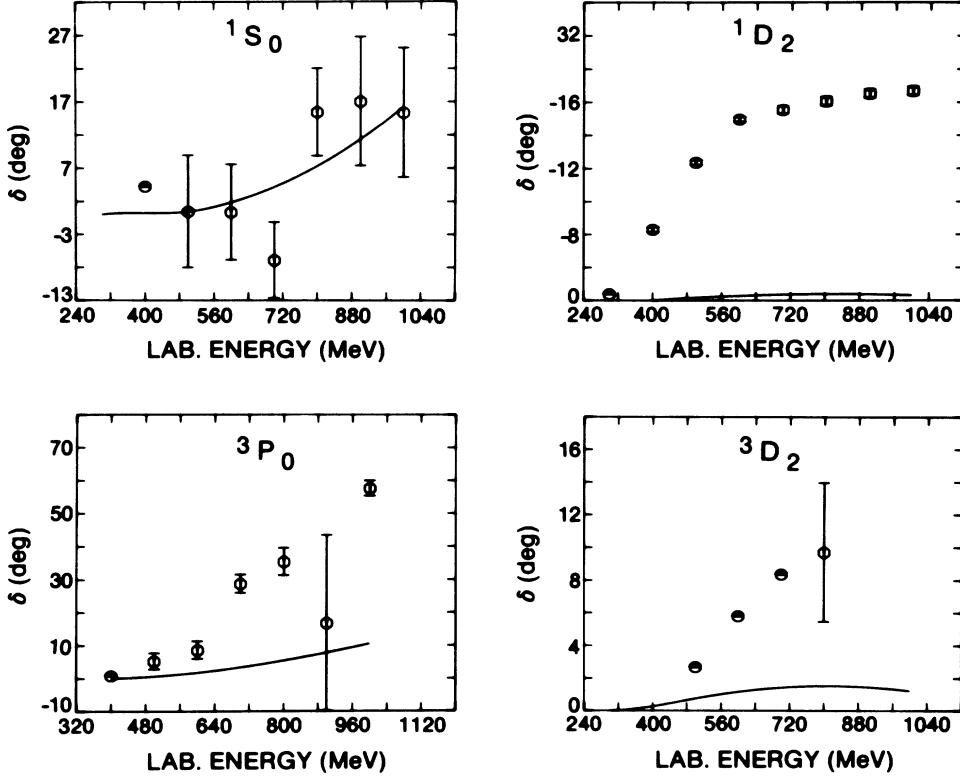


FIG. 9. NN inelasticity parameters ρ_{LSJ} in degrees (defined in the Arndt-Roper convention) as function of the nucleon lab energy derived from the unitary OBE model. The error bars are taken from Ref. 12.

V. SUMMARY

This is the first in a series of papers dealing with the extension of the Bonn meson exchange NN interaction above pion production threshold. Since the energy dependence of the time-ordered meson propagators leads to direct meson production nucleon (and Δ isobar) self-energy diagrams must now be included explicitly in order to still guarantee unitarity.

In this paper we describe the basic principles of including renormalization corrections in a realistic one-boson-exchange model. It is shown that, in our framework based on time-ordered perturbation theory, the independent iteration of (lowest order) bubble diagrams on both nucleon lines leads to dressing factors, which give well defined off-shell corrections to the meson exchange diagrams.

It is demonstrated that due to its short-range nature nucleon dressing provides additional attraction in lower partial waves, below and above pion threshold. A slight readjustment of meson parameters (especially a reduction of the value for the pion cutoff mass) leads to a reproduction of the empirical NN data below pion threshold which is of the same quality as before. The resulting inelasticities, however, are much too small compared to the empirical data. Nevertheless, with the use of energy-dependent meson propagators, nucleon dressing is required in order to have a unitary model above pion production threshold.

It is known that the bulk of the empirical inelasticities can be provided by including the Δ isobar decaying into N and π . The study of such an extended model for the NN interaction along the same guidelines as presented in this work will be the subject of a forthcoming paper. Also, the effect of noniterative stretched- and crossed-box diagrams remains to be investigated.

This work was supported in part by Deutsche Forschungsgemeinschaft.

APPENDIX A: EVALUATION OF h_α , Z_α , AND $R_{\alpha_1\alpha_2}$

Here, we evaluate explicitly the nucleon energy shift [Eq. (2.3)], the Z factor [Eq. (2.8)], and the dressing factor [Eq. (2.15)], in the two-nucleon c.m. system. The notation is displayed in Fig. 10.

Starting point is the π NN (renormalized) interaction matrix element

$$W_{\alpha'\alpha n}^{(\pi)} = - \frac{g_\pi}{[2\omega_{q-k}^{(\pi)}(2\pi)^3]^{1/2}} \times \bar{u}(\mathbf{q}, \lambda_{\alpha'}) i \gamma^5 u(\mathbf{k}, \lambda_\alpha) F_\pi[(\mathbf{q}-\mathbf{k})^2], \quad (\text{A1})$$

where $u(\mathbf{k}, \lambda_q)$ denotes the usual (positive-energy) Dirac spinor with $u^\dagger u = 1$, and

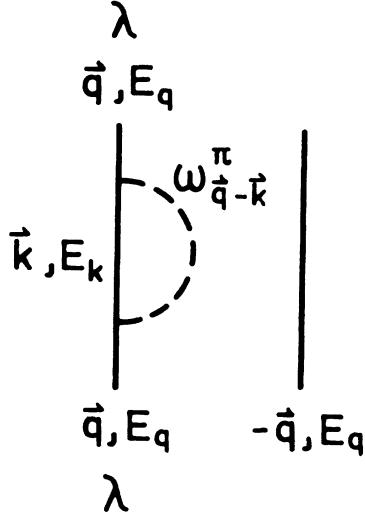


FIG. 10. Nucleon self-energy diagram displaying the notation as used in the text.

$$\omega_{q-k}^{(\pi)} \equiv [m_\pi^2 + (\mathbf{q} - \mathbf{k})^2]^{1/2}$$

is the relativistic pion energy. F_π is the π NN form factor, conventionally parametrized as

$$F_\pi = \frac{\Lambda_\pi^2 - m_\pi^2}{\Lambda_\pi^2 + (\mathbf{q} - \mathbf{k})^2}, \quad (\text{A2})$$

Λ_π being the cutoff mass. (The trivial isospin-dependence

$$\begin{aligned} B(q) &= \frac{3g_\pi^2}{(2\pi)^3} \int d^3k \frac{E_q E_k - m^2 - qk \cos\theta}{4\omega_{q-k}^\pi E_q E_k} F_\pi^2 \\ &= \frac{g_\pi^2}{4\pi} \frac{3}{4\pi E_q} \int_0^\infty dk \frac{k^2}{E_k} \int_{-1}^{+1} d \cos\theta (E_q E_k - m^2 - qk \cos\theta) (\omega_{q-k}^\pi)^{-1} F_\pi^2, \end{aligned} \quad (\text{A6})$$

where θ is the angle between \mathbf{q} and \mathbf{k} .

We then obtain for the energy shift

$$\frac{h_q(E_q)}{Z_q^2(E_q)} = \frac{g_\pi^2}{4\pi} \frac{3}{4\pi E_q} \int_0^\infty dk \frac{k^2}{E_k} \int_{-1}^{+1} d \cos\theta \frac{E_q E_k - m^2 - qk \cos\theta}{\omega_{q-k}^\pi (E_q - E_k - \omega_{q-k}^\pi)} F_\pi^2, \quad (\text{A7})$$

for the Z factor

$$\begin{aligned} Z_q^{-2}(E_q) &= 1 - I_q, \\ I_q &\equiv \frac{g_\pi^2}{4\pi} \frac{3}{4\pi E_q} \int_0^\infty dk \frac{k^2}{E_k} \int_{-1}^{+1} d \cos\theta \frac{E_q E_k - m^2 - qk \cos\theta}{\omega_{q-k}^\pi (E_q - E_k - \omega_{q-k}^\pi)^2} F_\pi^2, \end{aligned} \quad (\text{A8})$$

and for the dressing factor

$$\begin{aligned} R_q^{-2}(z) &= 1 - 2(z - 2E_q)\Gamma_q(z - E_q), \\ \Gamma_q(z - E_q) &= \frac{g_\pi^2}{4\pi} \frac{3}{4\pi E_q} \int_0^\infty dk \frac{k^2}{E_k} \int_{-1}^{+1} d \cos\theta \frac{(E_q E_k - m^2 - qk \cos\theta) F_\pi^2}{\omega_{q-k}^\pi (E_q - E_k - \omega_{q-k}^\pi)^2 (z - E_q - E_k - \omega_{q-k}^\pi)}. \end{aligned} \quad (\text{A9})$$

APPENDIX B: TREATMENT OF SINGULARITIES IN THE OBE POTENTIAL

In the two-nucleon c.m. system and helicity state basis the one-pion exchange potential (OPEP) is given by ($\mathbf{k} \equiv \mathbf{q}' - \mathbf{q}$)

is suppressed.)

We first calculate

$$B(\mathbf{q}) \equiv \sum_{\alpha'n} W_{\alpha\alpha'n}^{(\pi)} W_{\alpha'n}^{(\pi)}$$

appearing in all quantities to be considered. With Eq. (A1) we obtain

$$\begin{aligned} B(\mathbf{q}) &= \frac{g_\pi^2 \tau^2}{(2\pi)^3} \int d^3k \frac{1}{2\omega_{q-k}^\pi} \bar{u}(\mathbf{q}, \lambda) \\ &\quad \times i\gamma^5 \Lambda_+(\mathbf{k}) i\gamma^5 u(\mathbf{q}, \lambda) F_\pi^2. \end{aligned} \quad (\text{A3})$$

The factor $\tau^2=3$ is due to the isospin dependence. $\Lambda_+(\mathbf{k})$ is the projector on positive-energy nucleon states,

$$\Lambda_+(\mathbf{k}) = \frac{1}{2E_k} (\gamma^0 E_k - \boldsymbol{\gamma} \cdot \mathbf{k} + m) \quad (\text{A4})$$

[$E_k \equiv (k^2 + m^2)^{1/2}$, m the nucleon mass]. Equation (A3) can be simplified as

$$\begin{aligned} B(\mathbf{q}) &= \frac{3g_\pi^2}{(2\pi)^3} \int d^3k \frac{1}{2\omega_{q-k}^\pi} \bar{u}(\mathbf{q}, \lambda) \\ &\quad \times \frac{\gamma^0 E_k - \boldsymbol{\gamma} \cdot \mathbf{k} - m}{2E_k} u(\mathbf{q}, \lambda) F_\pi^2. \end{aligned} \quad (\text{A5})$$

Without loss of generality we put \mathbf{q} on the z axis and \mathbf{k} into the x-z plane, which leads to

$$\langle \mathbf{q}' \Lambda'_1 \Lambda'_2 | V_\pi(z) | \mathbf{q} \Lambda_1 \Lambda_2 \rangle = 2 \frac{g_\pi^2}{4\pi^2} \tau_1 \cdot \tau_2 \frac{1}{2\omega_k} \frac{\bar{u}(\mathbf{q}', \Lambda'_1) i \gamma^5 u(\mathbf{q}, \Lambda_1) \bar{u}(-\mathbf{q}', \Lambda'_2) i \gamma^5 u(-\mathbf{q}, \Lambda_2)}{z - E_{q'} - E_q - \omega_k + i\varepsilon}. \quad (\text{B1})$$

The resulting partial wave amplitudes have the following structure

$$\begin{aligned} V^J(q', q | z) &\sim \int_{-1}^{+1} dt \frac{f(q', q, t)}{z - E_{q'} - E_q - \omega_{q'qt} + i\varepsilon} \\ &= \mathcal{P} \int_{-1}^{+1} dt \frac{f(q', q, t)}{z - E_{q'} - E_q - \omega_{q'qt}} - i\pi \int_{-1}^{+1} dt \delta(z - E_{q'} - E_q - \omega_{q'qt}) f(q', q, t), \end{aligned} \quad (\text{B2})$$

where $t \equiv \cos\vartheta$, ϑ being the angle between \mathbf{q}' and \mathbf{q} . $f(q', q, t)$ is a well-defined function of q , q' , and t . For $z \geq 2m + m_\pi$ the principal value integral has a pole for

$$t_{\text{pol}} = \frac{m_\pi^2 + q'^2 + q^2 - (z - E_{q'} - E_q)^2}{2q'q} \quad (\text{B3})$$

which depends on both momenta q and q' . This pole may be removed by adding and subtracting the integral

$$\int_{-1}^{+1} dt \frac{(z - E_{q'} - E_q) f(q', q, t_{\text{pol}})}{\omega_{q'qt} (z - E_{q'} - E_q - \omega_{q'qt})} = \frac{(z - E_{q'} - E_q) f(q', q, t_{\text{pol}})}{q'q} \ln \frac{z - E_{q'} - E_q - \omega_{q'qt_+}}{z - E_{q'} - E_q - \omega_{q'qt_-}}, \quad (\text{B4})$$

where $t_\pm = \pm 1$. Then Eq. (B2) becomes

$$\begin{aligned} V^J(q', q | z) &\approx \int_{-1}^{+1} dt \frac{\omega_{q'qt} f(q', q, t) - (z - E_{q'} - E_q) f(q', q, t_{\text{pol}})}{\omega_{q'qt} (z - E_{q'} - E_q - \omega_{q'qt})} + \frac{(z - E_{q'} - E_q) f(q', q, t_{\text{pol}})}{q'q} \\ &\times \left[\ln \left| \frac{z - E_{q'} - E_q - \omega_{q'qt_+}}{z - E_{q'} - E_q - \omega_{q'qt_-}} \right| - i\pi\theta \left[-\frac{z - E_{q'} - E_q - \omega_{q'qt_+}}{z - E_{q'} - E_q - \omega_{q'qt_-}} \right] \right] \end{aligned} \quad (\text{B5})$$

(θ is the usual step function). The logarithmic term still contains singularities which depend not only on the starting energy z but also on the (off shell) momenta q and q' . They are located in a bounded region on the real axis with $q', q < q_0$ ($z \equiv 2E_{q_0}$).

In order to solve the equations in the presence of such singularities the path of integration is shifted into the complex plane by a well-defined mapping so that the contour does not meet any region of singularities.¹³

Since the logarithmic singularities of the pion propaga-

tor are located in a region $q', q < q_0$, the mapping

$$q \rightarrow q \left[2 - \frac{q}{q_0} \right] + i\beta \frac{q}{q_0} (q - q_0) \quad (\text{B6})$$

was chosen for $q', q \in (0, q_0)$. Note that on shell all momenta are real. Therefore no extra transformation must be performed to obtain a solution of the T -matrix equation for real momenta. In practice, values for β in the range between 1.2 and 0.8 turned out to be suitable.

*Also at Institut für Kernphysik der Kernforschungsanlage Jülich, D-5170 Jülich, Federal Republic of Germany.

¹R. Machleidt, K. Holinde, and Ch. Elster, Phys. Rep. **149**, 1 (1987).

²R. Vinh Mau, in *Mesons in Nuclei*, edited by M. Rho and D. H. Wilkinson (North-Holland, Amsterdam, 1979), Vol I, p. 151.

³M. J. Levine, J. Wright, and J. A. Tjon, Phys. Rev. **157**, 1416 (1967).

⁴S. J. Brodsky, Comments Nucl. Part. Phys. **12**, 213 (1984).

⁵T. D. Lee, Phys. Rev. **95**, 1329 (1954).

⁶D. Schütte and J. D. Providencia, Nucl. Phys. **A338**, 436 (1980).

⁷M. G. Fuda, Phys. Rev. C **25**, 1972 (1982).

⁸M. Sawicki and D. Schütte, Z. Naturforsch. **36A**, 1261 (1981).

⁹W. M. Kloet and R. R. Silbar, Nucl. Phys. **A338**, 281 (1980).

¹⁰E. van Faassen and J. A. Tjon, Phys. Rev. C **33**, 2105 (1986).

¹¹K. Erkelenz, Phys. Rep. **13C**, 193 (1974).

¹²R. A. Arndt *et al.*, Phys. Rev. D **28**, 97 (1983).

¹³W. Ebenhö, Nucl. Phys. **A191**, 97 (1972).

¹⁴K. Kotthoff, K. Holinde, R. Machleidt, and D. Schütte, Nucl. Phys. **A242**, 429 (1975).

¹⁵R. Dubois *et al.*, Nucl. Phys. **A377**, 554 (1982).

¹⁶E. van Faassen, Ph.D. thesis, Institute for Theoretical Physics, Utrecht, 1985.